Metrol. Meas. Syst., Vol. 27 (2020) No. 4, pp. 575–587
DOI: 10.24425/mms.2020.134839

PAN POLSKA AKADEMIA NAUK

METROLOGY AND MEASUREMENT SYSTEMS
Index 330930, ISSN 0860-8229
www.metrology.wat.edu.pl

M&MS

A SIMPLE AND AFFORDABLE POWERING CIRCUIT FOR IoT SENSOR NODES WITH ENERGY HARVESTING

Adam Bouřa

Czech Technical University in Prague, Department of Microelectronics, Technická 2 St., 166 27 Prague 6, Czech Republic (✉ *bouraa@fel.cvut.cz*, +420 224 352 335)

Abstract

The paper presents a circuit structure that can be used for powering an IoT (Internet of Things) sensor node and that can use energy just from its surroundings. The main advantage of the presented solution is its very low cost that allows mass applicability e.g. in the IoT smart grids and ubiquitous sensors. It is intended for energy sources that can provide enough voltage but that can provide only low currents such as piezoelectric transducers or small photovoltaic panels (PV) under indoor light conditions. The circuit is able to accumulate energy in a capacitor until a certain level and then to pass it to the load. The presented circuit exhibits similar functionality to a commercially available EH300 energy harvester (EH). The paper compares electrical properties of the presented circuit and the EH300 device, their form factors and costs. The EH circuit's performance is tested together with an LTC3531 buck-boost DC/DC converter which can provide constant voltage for the following electronics. The paper provides guidelines for selecting an optimal capacity of the storage capacitor. The functionality of the solution presented is demonstrated in a sensor node that periodically transmits measured data to the base station using just the power from the PV panel or the piezoelectric generator. The presented harvester and powering circuit are compact part of the sensor node's electronics but they can be also realized as an external powering module to be added to existing solutions.

Keywords: energy harvesting, energy management, Internet of Things, wireless sensor networks.

1. Introduction

Energy harvesting allows the operation of electronic devices without batteries or increases battery life. It is most suitable for situations in which standard powering cannot be applied or in which it is inconvenient to replace the battery. A typical application would be a sensor node that is located in an inaccessible place [1–4]. Unfortunately, alternative energy sources are usually weak and cannot provide enough energy for direct powering of the device (*e.g.* small PVs [5] or other energy generators [6]). The energy thus must be collected in a capacitor or an accumulator first, and afterwards it can be released to the load. These circuits are called *energy harvesters* (EH). Commercially available devices that can be used as EH exist, but their price is usually high

and thus they cannot be used for a large number of sensor nodes applications. This paper presents a circuit that works as an EH; it could be a compact part of the device, and its price allows mass applicability.

The paper presents a powering scheme that is based on periodical charging of the electrolytic capacitor and releasing it to the electronics of the sensor node. The solution presented avoids usage of the battery and/or accumulator, guaranteeing longer performance stability (no battery ageing [7]) and a wider range of possible temperatures [8, 9]. The sensor node is powered off most of the time while the energy is harvested into the storage capacitor. When it is fully charged, the energy is released. All functionalities such as wake-up procedures, measurement, data processing, encoding and transmission must thus be finished before the storage capacitor is discharged. The capacity of the storage capacitor is crucial and must be optimized. It must be large enough to fulfil the power requirements of the sensor node, while not being too large to minimize the charging time as much as possible. This paper presents a guideline on how to find the optimal capacity of the capacitor while taking into account the power consumption of the sensor node and real properties of the powering circuit. This paper has the following structure: Section 2 describes the EH circuit and compares the commercial harvester with an alternative circuit that can be part of the sensor node powering; Section 3 summarizes the efficiency of the LTC3531 buck-boost converter under different powering conditions and working together with the EH circuit; Section 4 presents the practical application of a sensor node that is powered by a small PV or piezoelectric generator.

2. Energy harvester

2.1. Energy harvester EH300

A representative example of a commercially available module is the EH300 harvester [10]. Its operational principle is as follows (see Fig. 1, left). The harvester EH300 stores the energy from the source, *e.g.*, a PV cell, in a 1000 μF capacitor while the load is disconnected. When it is charged to 3.6 V (V_H), the capacitor is connected to the output port and the accumulated energy is released to the load. The energy is available until the voltage on the capacitor drops down to 1.8 V (V_L) and then the EH's output is disconnected from the load. When the harvester's output is closed, the energy from the energy source can be harvested again. For a 1000 μF capacitor the

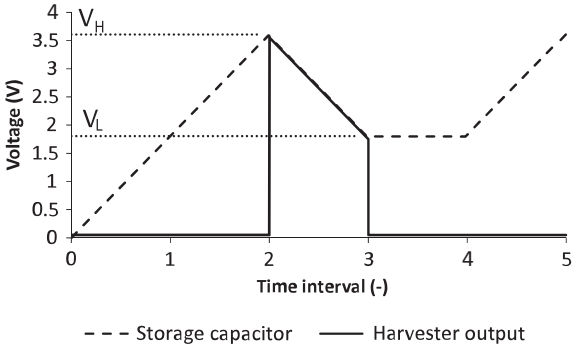

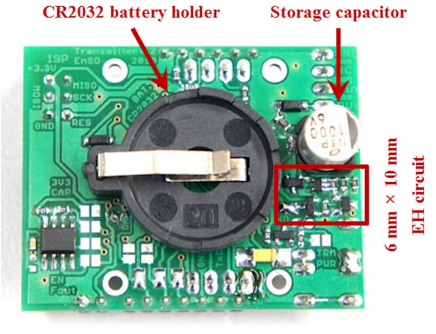

Fig. 1. Operating cycle of the harvester EH300 [2] (left). Bottom side of the sensor node developed with the harvesting circuit footprint (right).

Metrol. Meas. Syst., Vol. 27 (2020), No. 4, pp. 575–587
DOI: 10.24425/mms.2020.134839

energy released in one charging cycle is 4900 μJ according (1).

$$E_C = \frac{1}{2} \cdot C \cdot \left(V_H^2 - V_L^2\right). \tag{1}$$

Various energy sources can be used; solar panels, piezoelectric converters or other sources that can provide voltage greater than V_H and are able to cover the EH's power consumption. The self-consumption of the device is declared to be 200 nA at 4 V [10], though it was measured to be higher due to the storage capacitor's leakage current (see Section 2.4).

2.2. Alternative harvesting circuit

Figure 2 presents an alternative circuit structure that has the same basic functionality as the EH300. Energy is passed to capacitor C1 through a Graetz rectifier (D1–D4). The voltage is then compared to the voltage reference (R1, IC1) using the comparator (IC2). Next the comparator implements a hysteresis using resistors R2, R3 and R4. The comparator drives a SiP32431 chip [11]. It is a switch that has an ultra-low leakage and quiescent current and it connects the storage capacitor C1 to the load.

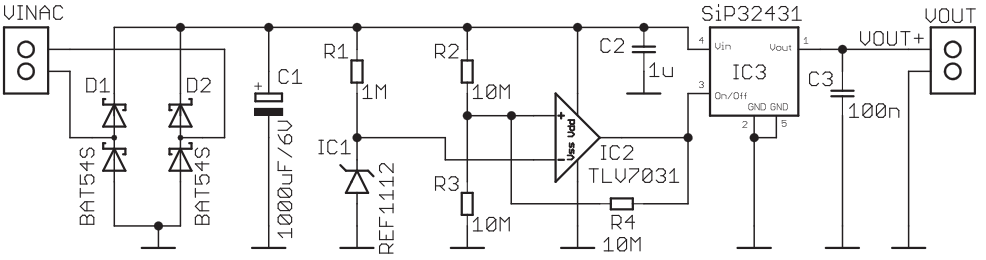

Fig. 2. Diagram of the alternative harvesting circuit.

The resistor values R2, R3, R4 and the voltage reference V_{ref} (IC1, R1) can be set to different voltage levels V_L and V_H to accommodate the hysteresis. Equations (2) and (3) define coefficients K1 and K2 that can be derived from the voltage divider R2, R3, R4 for a switched and released comparator, from the given reference voltage V_{ref} on its inverting input and demanded voltage levels V_H and V_L. The resistor values can be expressed by the following equations for any voltage levels V_L, V_H and optional resistor R1 (4).

$$K_1 = \frac{V_{ref}}{V_L} = \frac{R_1R_2 + R_2R_3}{R_1R_3 + R_1R_2 + R_2R_3}, \tag{2}$$

$$K_2 = \frac{V_{ref}}{V_H} = \frac{R_2R_3}{R_1R_3 + R_1R_2 + R_2R_3}, \tag{3}$$

$$R_1 = R; \qquad R_2 = \frac{RK_2}{1 - K_1}; \qquad R_3 = \frac{RK_2}{K_1 - K_2}. \tag{4}$$

In order to minimize power consumption, the resistors should be set as high as possible. For the given values in the diagram in Fig. 2, the operating voltage levels are similar to those of the EH300 device (1.875 V and 3.75 V). The steady leakage current of the circuit can be estimated from the diagram, taking into account in the quiescent currents of the devices (5).

$$I_{leak} = \frac{(V_{C1} - 1.25)}{R_1} + \frac{V_{C1}}{R_2 + R_3 \| R_4} + I_{TLV7031} + I_{C1}. \tag{5}$$

The quiescent current at the voltage reference is given by resistor R1 and should be at least 550 nA [12] for the minimal voltage 1.8 V. This is why resistor R1 is 1 MΩ. The voltage reference current is proportionally bigger for higher voltages on the capacitor. The voltage divider R2, R3, R4 loads the capacitor by a resistance of 15 MΩ and the quiescent current of the comparator is approximately 300 nA [13]. The leakage current of electrolytic capacitor C1 should always be lower than 3 μA [14], but it is dependent on the voltage when it is close to its rated voltage [15]. The maximal leakage current of the capacitor in the circuit was measured to be 700 nA at 3.5 V, 25 °C and rated voltage 6 V. The leakage currents of the other components are negligible. The total leakage current of the circuit (excluding the storage capacitor) varies between 1.05 μA and 3.05 μA depending on capacitor's actual voltage (that varies between 1.875 V and 3.75 V). The total leakage current can be higher due to leakage of the storage capacitor (see Section 2.3).

2.3. Storage capacitor

The storage capacitor should be large enough to provide energy to the sensor node. The minimum capacity is around 100 μF (see Section 3.2) and the typical capacity is about 1000 μF. This means that the capacitor is usually electrolytic which induces problems with the leakage current. The storage capacitor's leakage current can represent a significant portion of the harvester's total power consumption. Specifically, it depends on temperature, actual voltage, forming characteristics, time, and total capacity [15, 16].

To minimize the leakage, it is important to follow the following principles:

- the capacity should be optimal for the given application (*e.g.*, not too large),
- a high-quality capacitor should be used (*e.g.*, low leakage series),
- a high temperature rate capacitor should be used,
- a high voltage rating capacitor should be used as the leakage current increases exponentially when the operating voltage exceeds the rated voltage and approaches the forming voltage,
- the capacitor should be new or well formatted (older capacitors should be treated for least 24 hours at the maximal rated voltage).

When the electrolytic capacitor is charged by a high current peak, the leakage current is initially very high and slowly decreases over time to its steady value (Curie–von Schweidler law). This effect should be taken into account when the high current impulses are harvested.

2.4. Comparison of the harvesters

The circuit presented and the commercial harvester EH300 differ in their leakage currents which must be covered by the harvested energy source. The leakage currents were measured and calculated indirectly from the voltage drop on the capacitor (Fig. 3 top, left). The storage capacitors were charged to a voltage of 3.5 V and then self-discharge of the circuit was checked using the voltmeter with input impedance 200 GΩ and input bias current lower than 1 nA. The leakage current was calculated from the voltage drop ΔV_C between two consecutive measurements with time difference ΔT using the (6) – see Fig. 3 top, right.

$$I_{leak} \approx \frac{\Delta V_C \cdot C}{\Delta T} . \tag{6}$$

The leakage current can be also recalculated to a function of the actual voltage on the capacitor V_C (Fig. 3 bottom, left). There are two observable regions of the characteristics (see dash lines in Fig. 3 bottom, left). When the capacitor is charged to the maximum, the leakage current is high due to the effect of the high transient charging current (dash line 1 in Fig. 3 bottom, left). Also, it is higher because the voltage is closer to the capacitor's rated voltage. When the capacitor's

Metrol. Meas. Syst., Vol. 27 (2020), No. 4, pp. 575–587
DOI: 10.24425/mms.2020.134839

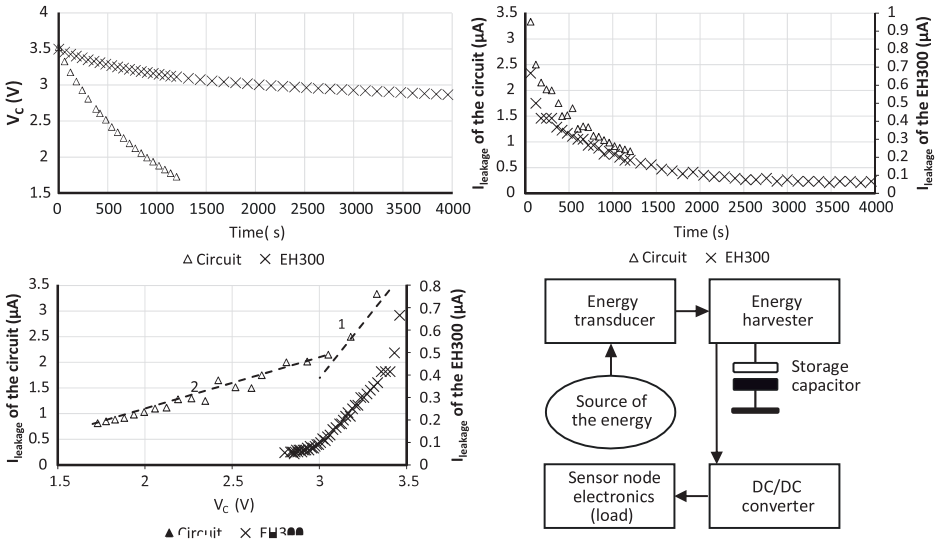

Fig. 3. Measurement of voltage drop on the storage capacitor over time caused by the leakage currents (top, left). Leakage currents of the devices calculated from the voltage drop (top, right). Comparison of the presented circuit and harvester EH300 leakage currents versus the actual voltage on the capacitor with effect of high leakage current due to a high charging current (bottom left). Block diagram of the IoT sensor node powering (bottom, right).

leakage is stabilized to its minimum, the leakage of the circuit structure takes the dominant role (dash line 2 in the figure).

It is evident from the data that the maximum leakage current of the presented circuit is approximately 3.3 μA at 3.5 V, which is 5 times bigger than the maximum leakage of the EH300. Moreover, an interesting result of the measurement is the fact that the real leakage of the EH300 is about 700 nA at 3.5 V, which is 3.5 times more than stated in the datasheet. The maximal leakage current of the harvester EH300 is stated to be 200 nA, but it is higher probably due to the transient effect in the storage capacitor.

Another important parameter for comparison are dimensions. Figures 1 right and 7 present a developed sensor node with the harvesting circuit. It is a compact part of the electronics and it occupies just 6 mm × 10 mm while the module EH300 is 11 times bigger (48 mm × 14 mm) and must be connected as an external module [10].

A further important parameter is the price of the components. The presented harvesting circuit consists of inexpensive standard components. The greater leakage current of the circuit compared to the EH300 is thus compensated for by a total component price that is 1/30th of that of the EH300 (2.3 € vs. 70 € at mouser.com). It allows wide spread applicability of the circuit in the IoT smart grids where the harvested energy is able to cover the leakage and also provide useful energy to the system. Table 1 presents a comparison of the key properties discussed.

Table 1. Comparison of the key properties.

Parameter	EH300	Circuit
Leakage current	< 0.7 μA	< 3.6 μA
Footprint	48 mm × 14 mm	6 mm × 10 mm
Price	~70 €	~2.3 €

3. DC/DC converter

As laid out in Section 2.1, the voltage from the energy harvester varies between 1.8 V and 3.6 V. This voltage must be stabilized for correct operation of sensor node electronics. This paper deals with a sensor node that is powered with 3 V and the voltage adjustment by the LTC3531 buck-boost DC/DC converter. The block diagram in Fig. 3 bottom, right describes the sensor node powering strategy. Alternative energy is converted to electrical energy in a proper transducer (PV, piezoelectric crystal, *etc.*). This energy is collected by the EH to the storage capacitor and when it is fully charged, the storage capacitor is connected to the DC/DC converter's input, providing a stabilized voltage for the load (sensor node's electronics).

3.1. Basic parameters of LTC3531

The LTC3531 is a synchronous buck-boost DC/DC converter that operates from input voltages above, below or equal to the output voltage. It was connected according to the datasheet [17] and implemented in the powering of the sensor node (Fig. 4 left and Fig. 7).

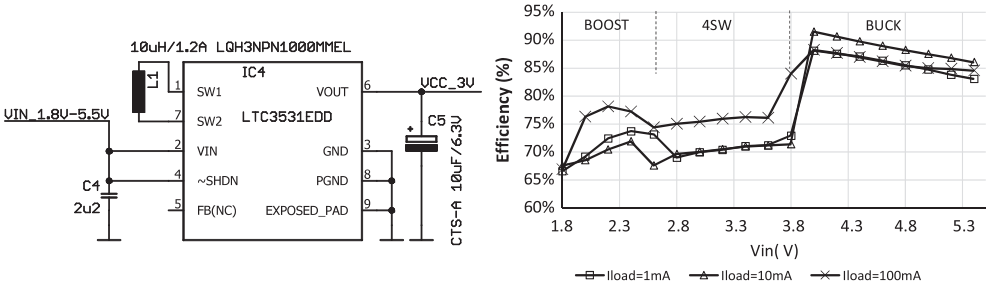

Fig. 4. Diagram of the DC/DC converter (left). Efficiency of the DC/DC converter versus input voltage and loading current. The converter's operation modes are marked by the vertical dash lines. Compare with [17] (right).

Considering the 3.0 V output voltage, the converter works as a BOOST for input voltages from 1.8 V to 2.6 V in the 4-Switch Mode for input voltages from 2.6 V to 3.8 V and as a BUCK converter for input voltages from 3.8 V to 5.5 V. The efficiency of the conversion depends upon the operation mode and loading current. Fig. 4 right presents the efficiency measurement for a given sample that is used in the sensor node. The measurement results are similar to the datasheet specifications. The slightly lower efficiency observed is probably caused by higher resistance of the coil and non-ideal physical implementation on the *printed circuit board* (PCB).

The converter is used only in BOOST and 4-Switch Modes in the presented application because of the voltage levels from the harvester. This is why the efficiency is typically between 65% and 75% depending on the loading current. The power consumption of the unloaded converter was measured to be approximately 60 μW.

Beside the steady efficiency of the converter, it is also important to know how much energy is needed for its start-up. It is especially important in the presented powering scheme, wherein the total energy is limited by the harvester's storage capacitor C1 (in Fig. 2). Every time the harvester releases the energy to the DC/DC converter, some portion of it is used for the converter's start-up and for charging the filtering capacitor C5 (in Fig. 4 left). It is useful only when the capacitor is charged to 2.7 V ~3.0 V, which is the necessary voltage for the correct operation of the sensor node. This is why capacitor C5 should be as small as possible so as not to waste the energy that

Metrol. Meas. Syst., Vol. 27 (2020), No. 4, pp. 575–587
DOI: 10.24425/mms.2020.134839

is lost when the output voltage fades away. The optimal capacity is 10 μF which is a compromise between the start-up energy and the output voltage ripple.

Figure 5 left presents the input (V_C) and output (V_{load}) voltages of the converter during the start-up while the converter is slightly loaded through a 2.2 kΩ resistor. At 0 μs, it is connected to the 220 μF capacitor that is charged to 3.6 V. After approximately 50 μs, the output voltage starts to rise and then it reaches the final value of 3.0 V. The start-up time of the converter is approximately 250 μs, and during this period the storage capacitor's voltage drops to 3.2 V. The start-up energy is thus about 300 μJ (1).

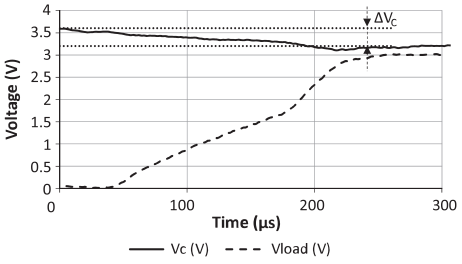

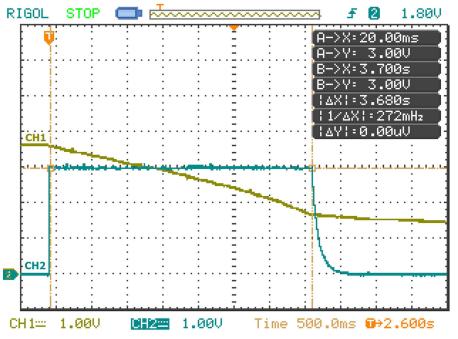

Fig. 5. Startup of the DC/DC converter that is loaded through a 2.2 kΩ resistor and connected to a 220 μF capacitor that is charged to 3.6 V (left). Typical example of the sensor node powering. Channel 1 shows the voltage on the 1000 μF storage capacitor that was connected to the converter loaded through a 10 kΩ resistor. Channel 2 shows the load's voltage (right).

3.2. Performance of DC/DC converter with EH

The typical performance of the DC/DC converter with the energy harvester is presented in Fig. 5 right. When the storage capacitor is connected to the converter's input, the converter starts to operate while the storage capacitor is being discharged (CH1 – yellow curve in Fig. 5 right). After the start-up time of 250 μs (see the detail in Fig. 5 left), the converter provides a stabilized voltage of 3 V to the electronics. The sensor node is in the active mode until the harvester circuit switches off the converter's input voltage and the stabilized output drops to zero (CH2 – blue curve in Fig. 5 right).

The active time of the node is determined by the capacity of the storage capacitor and loading current. The minimum capacity of storage capacitor C1 is given by the start-up energy of the converter, which was measured to be 300 μJ, and for given voltage levels from 1.8 V to 3.6 V, it is approximately 60 μF. The minimum capacity of the storage capacitor is thus approximately 100 μF. Nevertheless, to cover the typical performance of the sensor node the storage capacitor must generally have a much larger capacity, typically more than 1000 μF. Table 2 presents the active time of the sensor node for a storage capacitor of 1000 μF and different loading currents on the converter's output. The efficiency presented in the table is determined by the ratio between the energy that is delivered to the load and the energy that is released from the capacitor during the operating cycle (4900 μJ). The EH's leakage current is omitted here. For very weak loads, the efficiency of the converter is affected by the start-up energy of 300 μJ and power consumption of the converter (60 μW). This is typical when sensor needs to stabilize its performance after start-up. For higher loading currents (when the IoT node is in the active mode), the efficiency is determined mostly by the converter's performance and is between 66% and 74% (Fig. 6 left).

Table 2. Measurement of the active mode time for the storage capacitor 1000 μF and different load on the converter's output.

Rload	Iload	Active mode time	Energy delivered to the load	Efficiency
10 MΩ	0.3 μA	76 s	68 μJ	1.39%
1 MΩ	3 μA	65 s	585 μJ	11.9%
100 kΩ	30 μA	25 s	2250 μJ	45.9%
10 kΩ	300 μA	3.62 s	3260 μJ	66.5%
1.5 kΩ	2000 μA	0.56 s	3360 μJ	69.6%

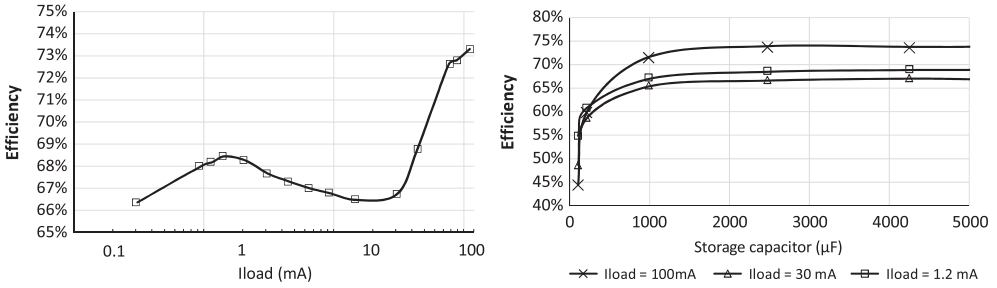

Fig. 6. Efficiency of delivering energy from the storage capacitor 1000 μF to the load through the DC/DC converter as a function of the loading current (left). Measurement results of energy transfer efficiency from the storage capacitor to the load through the DC/DC converter for different loading currents and storage capacitors (right).

As mentioned above, in many applications it is important to have a longer start-up time to steady the sensors' performance (*e.g.*, a humidity sensor [18], electrochemical sensors [19] *etc.*). In these cases, the sensor node electronics must be set to idle mode to wait for the start-up of all the peripheries. This procedure consumes some of the energy from the storage capacitor, and thus it should be reflected in the design (Section 4.1).

Figure 6 right shows the measurements results of delivering the energy to the load for different loading currents and for different storage capacitors. There is evidently a clear linear character for the capacities above 1000 μF. For smaller capacitors, the converter's start-up energy affects this linear character and sharply decreases the efficiency of the powering.

4. Application example

4.1. Storage capacitor estimation

As was already mentioned, the storage capacitor of the harvester must have the optimal capacity. It must be able to provide enough energy to the sensor node, but it should not be too large so as to keep the charging cycles short. The powering scheme presented requires periodical discharging the storage capacitor below the voltage level V_L. The active operation mode thus must be followed by the steady mode wherein the sensor node's electronics load the EH to waste the rest of the storage capacitor's energy. This is why the capacity of the storage capacitor should be just a bit larger than the minimal needed value. The minimal value can be estimated from the knowledge of the sensor node's power consumption during the idle mode time (time needed for start-up of the sensors and other peripheries) and the power consumption during the active mode

Metrol. Meas. Syst., Vol. 27 (2020), No. 4, pp. 575–587
DOI: 10.24425/mms.2020.134839

time (measurement, data processing, data transmission, *etc.*). The optimal value is slightly larger than the minimal value and it is important to know the following parameters to find it.

C_{EH} (F) – Storage capacitor's capacity.
$C_{\min}$ (F) – Minimal capacity of the storage capacitor.
E_A (J) – Energy needed for the active mode period.
E_C (J) – Storage capacitor's energy that is released during the EH's charging cycle (1).
$E_{C\,\min}$ (J) – Total minimal energy needed for the sensor node's operation (8).
E_I (J) – Energy needed for the idle mode period.
E_S (J) – Converter's start-up energy.
I_A (A) – Average current to the sensor node's electronics during the active mode.
I_I (A) – Average current to the sensor node's electronics during the idle mode when larger than 5 μA – see below.
I_L (A) – Upper estimate of the EH's leakage current.
η_A (–) – Efficiency of the converter that is loaded by I_A.
η_I (–) – Efficiency of the converter that is loaded by I_I.
P_A (W) – Average power consumption during the active mode, $P_A = V_{CC} \cdot I_A$.
P_I(W) – Average power consumption during the idle mode, $P_I = V_{CC} \cdot I_I$.
P_L (W) – Upper estimate of power losses caused by leakage current, $P_L = I_L \cdot V_H$.
P_{SC} (W) – Power consumption of the unloaded DC/DC converter.
T_A (s) – Active mode time of the sensor node.
T_I(s) – Idle mode time needed for the sensors' and peripheries' start-up.
V_{CC} (V) – Stabilized output voltage from the DC/DC converter.
V_H (V) – Maximal voltage on the EH's storage capacitor (see Section 2.1).
V_L (V) – Minimal voltage on the EH's storage capacitor (see Section 2.1).

The minimal capacity of the storage capacitor can be found using (7), which relates the EH's voltage levels and minimal total energy needed for the sensor node's operation. This minimal energy is given by (8) and is the sum of the converter's start-up energy, the energy needed during the idle mode period and the energy needed during the active mode period. The idle mode time can be relatively long, and thus the EH's leakage current and converter's power consumption can also have an effect during this period (9).

$$C_{\min} = \frac{2 \cdot E_{C\,\min}}{V_H^2 - V_L^2}, \tag{7}$$

$$E_{C\,\min} = E_S + E_I + E_A, \tag{8}$$

$$E_I = T_I \cdot \left(\frac{P_I}{\eta_I} + P_{SC} + P_L \right), \tag{9}$$

$$E_A = T_A \cdot \left(\frac{P_A}{\eta_A} + P_{SC} + P_L \right) \approx T_A \cdot \frac{P_A}{\eta_A}, \tag{10}$$

$$C_{EH} > \frac{2 \cdot \left[T_I \cdot \left(\frac{V_{CC} \cdot I_I}{\eta_I} + P_{SC} + I_L \cdot V_H \right) + T_A \cdot \frac{V_{CC} \cdot I_A}{\eta_A} + E_S \right]}{V_H^2 - V_L^2}. \tag{11}$$

For current I_I lower than 5 μA the converter's power consumption P_{SC} is dominant and thus the current can be neglected in the equation (9). On the other hand, as the active mode is usually

short, the leakage current I_L and P_{SC} can be neglected in (10). Combining the equations, the expression for the EH capacitor can be found and is given by (11) relating the average current consumptions and relevant converter's efficiencies. These efficiencies can be found in Table 2 and Fig. 6 left. The active mode period can consist of several time intervals with widely varying current consumptions. This necessitates splitting the total energy E_A into relevant energy portions with appropriate efficiencies. Nevertheless, for a rough estimation, just the average current consumption and the worst-case efficiency can be taken into account. The following section presents the sensor node that performs basic functionality, managed with a 1000 μF storage capacitor.

4.2. Demonstration with sensor node

Figure 7 presents a developed sensor node that is able to wirelessly transmit measured data (*e.g.* temperature and humidity) to the receiver. The node uses a narrow band radio transceiver at ISM frequency 433 MHz. It can transfer the measured data to the base station with a data rate of up to 10 kbps and to a distance of up to 1 km [20] (It was successfully tested for 2.5 kbps and a distance greater than 250 m in a noisy urban area, using the presented harvesting circuit, 1000 μF storage capacitor and powered from a small solar cell according to Fig. 7).

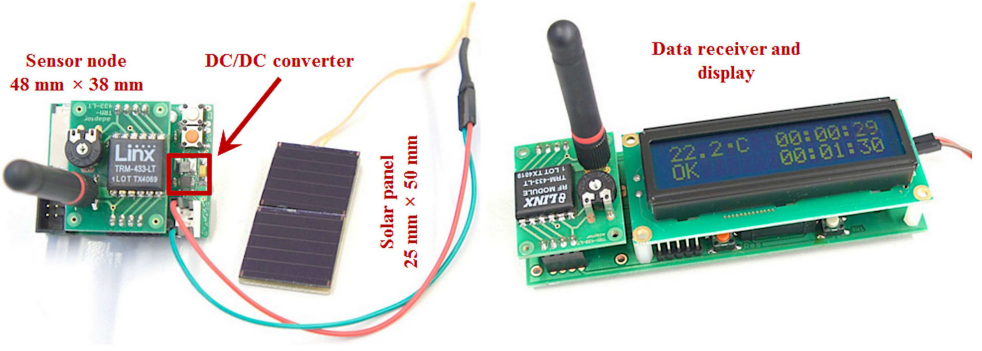

Fig. 7. Developed sensor node with energy harvesting circuit and the receiver.

The presented harvesting circuit is a compact part of the electronics and it occupies just 6 mm × 10 mm. It was tested with a small amorphous photovoltaic panel SOLEMS that is can be operated even in a very low-light environment. When the device is powered only from a PV of dimensions 5 cm × 2.5 cm, the data transmission rate is every 19 seconds for high intensities of light (8000 lx) and decreases to every 2 hours for a very dark environment (the panel is able to provide 6.7 μA, 4 V at 50 lx illumination). The node was also successfully tested with the piezoelectric transducer glued to a vibrating cantilever. Specifically, the transducer was glued to an 80 mm long and 25 mm wide beam made of 1.5 mm thick FR4 which was loaded with a 10 g seismic weight, and vibrated at 50 Hz with an amplitude of 0.5 mm. Under these conditions, it was able to charge the EH circuit every 6 minutes.

The developed node can use only the harvested energy or it can be also supported by a CR2032 battery (*e.g.* for long-term biasing of the sensor). The sensors' powering is separated from the DC/DC converter's output through a Schottky diode, and thus the battery can provide the biasing voltage even when the EH is switched off. When the EH turns on the powering, the electronics first check for the presence of a battery and according to the result, the correct operation mode is selected. If a battery is detected, the sensor node enters the active mode immediately; otherwise the

idle mode is entered first to steady the sensors. The capacity of the storage capacitor was calculated for this node according (11) with the following input parameters: V_{CC} = 3 V, V_H = 3.6 V, V_L = 1.8 V, T_I = 2 s, I_I = 70 μA, η_I = 0.46, P_{SC} = 60 μW, I_L = 3.5 μA, T_A = 82 ms, I_A = 9 mA, η_A = 0.67, E_S = 300 μJ. The resulting minimal capacity is 960 μF and thus the 1000 μF capacitor was assembled.

5. Conclusions

This paper presents a circuit structure that can be used as an energy harvester. Its functionality is similar to the commercially available EH300 harvester. The electrical parameters are worse concerning the leakage current of the circuit that should be covered by the harvested energy source. The worse parameters are compensated for by its very low price and compact footprint that allows mass applicability in IoT smart grids and networks where the nodes are operated just by the energy harvested from their surroundings. The presented harvester and powering circuit are compact part of the sensor node's electronics but they can be also realized as an external powering module to be added to existing solutions and ubiquitous sensor modules.

The performance of the harvester is affected by the voltage converter that stabilizes the powering voltage for the electronics. It was presented with the LTC3531 buck-boost converter as the stabilizer. Its efficiency varies between 65% and 73% depending on loading current. This paper also presents guidelines for selecting the optimal capacity of the storage capacitor according to the expected load.

The presented solution's functionality was proved on the developed sensor node which transmits measured data to the base station using only the power from the PV cell. The device can operate even in a very dark environment with an illuminance lower than 50 lx. Its functionality was also demonstrated using the piezoelectric generator which harvested vibrational energy at 50 Hz.

Acknowledgements

Research described in the paper has been supported by the project EnSO, Electronic Components and Systems for European Leadership Joint Undertaking in collaboration with the European Union's H2020 Framework Programme (H2020/2014-2020) and National Authorities, under grant agreement n° 692482. The research also was partly supported by the 7D – Eurostars grant n° 7D19001 – SACON – Smart Access Control for Smart Buildings.

References

[1] Dziadak, B., Makowski, Ł., & Michalski, A. (2016). Survey of energy harvesting systems for wireless sensor networks in environmental monitoring. *Metrology and Measurement Systems, 23*(4), 495–512. https://doi.org/10.1016/10.1515/mms-2016-0053

[2] Verma, A., Prakash, S., Srivastava, V., Kumar, A., & Mukhopadhyay, S. C. (2019). Sensing, Controlling, and IoT Infrastructure in Smart Building: A review. *IEEE Sensors Journal, 19*(20), 9036–9046. https://doi.org/10.1109/JSEN.2019.2922409

[3] Wang, Y., Rajib, S. S. M., Collins, C., & Grieve, B. (2018). Low-Cost Turbidity Sensor for Low-Power Wireless Monitoring of Fresh-Water Courses. *IEEE Sensors Journal, 18*(11), 4689–4696. https://doi.org/10.1109/JSEN.2018.2826778

[4] Li, J., Reiffs, A., Parchatka, U., & Fischer, H. (2015). In situ measurements of atmospheric CO and its correlation with NOx and O3 at a rural mountain site. *Metrology and Measurement Systems, 22*(1), 25–38. https://doi.org/10.1515/mms-2015-0001

[5] Labouret, A., & Villoz, M. (2010). *Solar Photovoltaic Energy (Let Renewable Energy)* (4th ed.). The Institution of Engineering and Technology.

[6] Chong, Y. W., Ismail, W., Ko, K., & Lee, C. Y. (2019). Energy harvesting for wearable devices: A review. *IEEE Sensors Journal*, 19(20), 9047–9062. https://doi.org/10.1109/JSEN.2019.2925638

[7] Leng, F., Tan, C. M., & Pecht, M. (2015). Effect of temperature on the aging rate of Li ion battery operating above room temperature. *Scientific reports , 5*, 12967. https://doi.org/10.1038/srep12967

[8] Wang, H., Xia, D., Si, N., Tao, Z., Fu, Y., Xiao, H., ... & Dena, S. (2018, August). Impact of Ambient Temperature on the Consistency of Lithium ion Batteries. *Proceedings of the 2018 International Conference on Sensing, Diagnostics, Prognostics, and Control (SDPC)*, China, 763–766. https://doi.org/10.1109/SDPC.2018.8664960

[9] Kuparowitz, M., Sedlakova, V., & Grmela, L. (2017). Leakage Current Degradation Due to Ion Drift and Diffusion in Tantalum and Niobium Oxide Capacitors. *Metrology and Measurement Systems, 24*(2), 255–264. https://doi.org/10.1515/mms-2017-0034

[10] Advanced Linear Devices, Inc. (2015). *EH300/301 EPAD®ENERGY HARVESTING™ MODULES*. [Datasheet, Vers. 2.2]. http://www.aldinc.com/pdf/EH300.pdf

[11] Vishay Intertechnology, Inc. (2020). *SiP32431DN, SiP32431DR, SiP32432DN, SiP32432DR*. [Datasheet, Rev. G], https://www.vishay.com/docs/66597/sip32431.pdf

[12] Texas Instruments Inc. (2018). *REF1112 10ppm/°C, 1-μA, 1.25-V Shunt Voltage Reference*. [Datasheet, Rev. D]. http://www.ti.com/lit/ds/symlink/ref1112.pdf

[13] Texas Instruments Inc. (2019). *TLV703x and TLV704x Small-Size, Nanopower, Low-Voltage Comparators*. [Datasheet, Rev. E]. http://www.ti.com/lit/ds/symlink/tlv7031.pdf

[14] Nichicon. (2019). *Aluminum electrolytic capacitors*. [Datasheet]. https://cz.mouser.com/datasheet/2/293/e-wt-30307.pdf

[15] Ragni, L. (2012). Unexpected dielectric behavior in aluminum wet electrolytic capacitors. *IEEE Transactions on Dielectrics and Electrical Insulation, 19*(1), 291–297. https://doi.org/10.1109/TDEI.2012.6148530

[16] Galla, S., Szewczyk, A., & Lentka, Ł. (2019). Electrochemical capacitor temperature fluctuations during charging/discharging processes. *Metrology and Measurement Systems, 6*(1), 23–35. https://doi.org/10.24425/mms.2019.126338

[17] Linear Technology Corporation. (2006). *LTC3531/LTC3531-3.3/LTC3531-3 200mA Buck-Boost Synchronous DC/DC Converters*. [Datasheet, Rev. B]. https://www.analog.com/media/en/technical-documentation/data-sheets/3531fb.pdf.

[18] MaxDetect Technology Co., Ltd. *Digital relative humidity & temperature sensor RHT03*. [Datasheet]

[19] Yin, H., Mu, X., Li, H., Liu, X., & Mason, A.J. (2018). CMOS Monolithic Electrochemical Gas Sensor Microsystem Using Room Temperature Ionic Liquid. *IEEE Sensors Journal, 18*(19), 7899–7906. https://doi.org/10.1109/JSEN.2018.2863644

[20] Linx Technologies. (2015). *LT Series Transceiver Module Data Guide*, [Datasheet]. https://linxtechnologies.com/wp/wp-content/uploads/trm-fff-lt.pdf

Adam Bouřa was born in Ostrava, Czechoslovakia, in 1980. He graduated in Microelectronics from the Faculty of Electrical Engineering, Czech Technical University in Prague in 2004. He received his Ph.D. degree in Electronics from FEE-CTU in 2012. Since January 2005 to February 2006 he was part-time research fellow and since February 2006 he has been an assistant professor at the Department of Microelectronics, FEE – CTU in Prague. His work is focused on wireless sensor systems, energy harvesting and microsystems.